Quantitative insights into electrostatics and structure of polymer brushes from microslit electrokinetic experiments and advanced modelling of interfacial electrohydrodynamics

Ralf Zimmermann, Jerome F. L. Duval, Carsten Werner, James Sterling

Quantitative insights into electrostatics and structure of polymer brushes from microslit electrokinetic experiments and advanced modelling of interfacial electrohydrodynamics

Ralf Zimmermann,[1,*] Jérôme F. L. Duval,[2] Carsten Werner,[1,3] James D. Sterling[4]

[1] Leibniz Institute of Polymer Research Dresden, Max Bergmann Center of Biomaterials Dresden, Hohe Str. 6, 01069 Dresden, Germany.

[2] CNRS-Université de Lorraine, Laboratoire Interdisciplinaire des Environnements Continentaux (LIEC), UMR 7360 CNRS, 15 avenue du Charmois, F-54500 Vandœuvre-lès-Nancy, France.

[3] Technische Universität Dresden, Center for Regenerative Therapies Dresden, Tatzberg 47, 01307 Dresden, Germany.

[4] Riggs School of Applied Life Sciences, Keck Graduate Institute, 535 Watson Drive, Claremont 91711, CA, USA

*corresponding author

Contact:

- Ralf Zimmermann

phone: +49 351 4658 258, fax: +49 351 4658 533, e-mail: zimmermn@ipfdd.de

- Jérôme F. L. Duval

phone: +33 3 72 74 47 20, e-mail: jerome.duval@univ-lorraine.fr

- Carsten Werner

phone: +49 351 4658 531, e-mail: werner@ipfdd.de

- James D. Sterling

phone: +1 909 607 9253 e-mail: jim_sterling@kgi.edu

Key words

Polymer brushes, electrohydrodynamics, streaming current, surface conductivity, ion pairing, self-consistent field theory, molecular dynamic simulations, dielectric decrement, born forces

Abstract

Polymer brushes are widely applied to modify and functionalize material surfaces. Fundamental understanding of polymer brush properties was achieved with the development of polymer theories and by the application of physico-chemical methods. The development of electrohydrodynamic formalisms for soft surfaces enabled major progress in the quantitative interpretation of streaming current and surface conductivity data collected for polymer brushes. In this paper, we review the basics of the methodology adopted for the analysis of interfacial charging and structure of polymer brushes, and illustrative examples of practical interest are discussed. In particular, we demonstrate how the combination of self-consistent field (SCF) and soft surface electrokinetic theories using Poisson-Boltzmann (PB) formulations allow the evaluation of the segment density distribution within poly(ethylene oxide) (PEO) brushes beyond the resolution limits of neutron reflectivity. The application of the methodology for the analysis of the charge, structure, and pairing with chaotropic anions is illustrated for strong cationic poly(2-(methacryloyloxy)ethyltrimethylammonium chloride) (PMETAC) brushes. Finally, we report refinements of the PB theory account for ion hydration, ion pairing, and dielectric decrement in brushes and we present an example of glycosaminoglycan (GAG) brushes where those effects are significant.

1. Introduction.

End-grafting of polymers is a widely applied method for tuning the properties of material surfaces [1], [2], [3]. At sufficiently high grafting densities, the polymers stretch away from the supporting surface and form a brush [4]. Nowadays, a wide variety of methods is available to control both the density and thickness of brushes [5]. Given the broad spectrum of available polymers, brush-coatings allow an unprecedent control over the surface properties and functionalities of particulate and planar material surfaces [3], [5]. Accordingly, polymer brushes are used in many application fields, including control of wetting [6] and lubrication [7], protein-resistant [8],[9] and antibacterial coatings [10], drug delivery [11], biosensing [12], and energy conversion and storage [13]. Responsive polymers allow the preparation of brushes that undergo dynamic changes in their conformation and properties triggered by an external stimulus such as pH, ionic strength, temperature, light, mechanical stress [14], or application of an external electric field. These 'smart responsive polymers' are used, for example, to control the hydrodynamic flow in nanopores [15] and microfluidic channels [16]. These options further opened up new avenues to develop smart devices [15], [16] and to mimic biological functions [17]. As an illustration, polymer brushes doped with gold-nanoparticles provide new perspectives for the design of colorimetric thin film sensors [18].

The broad application of polymer brushes was supported by the ongoing development of polymer theories [19], [20], [21], [22], [23], [24], [25], [26], [27], [28]. In their pioneering work, Alexander [21] and de Gennes [22], [23] considered brushes with a homogeneous density of monomers (box model). This assumption implies that all polymer chains are uniformly stretched [20]. Considering the most probable polymer configuration, Milner at al. evaluated parabolic brush density profiles applying the analytical self-consistent field (aSCF) theory [24]. Numerical self-consistent field (nSCF) theories account for fluctuations around the most probable polymer configuration, thus predicting a gradual decrease of the polymer density in the outermost region of the brush [25], [26], [27]. Molecular details of brush structures under various physiochemical medium conditions were further addressed with help of Monte Carlo [29] and molecular dynamic simulations [30].

Polyelectrolytes (PE) provide versatile options to prepare responsive brushes due to their ability to change their conformation upon changing electrolyte composition. The presence of ionized groups along the polymer backbone additionally contributes to the total free energy of the brush and thus to the brush conformation and properties [19]. Fundamental properties of weak and strong polyelectrolyte brushes were studied on the basis of scaling theories [31],[32],[33]. Zhulina et al. [33] developed an aSCF theory for polymer brushes consisting of

weakly charged pH-sensitive (annealing) polyelectrolytes. The approach allowed a detailed analysis of the local degree of chain ionization, of the resulting electrostatic potential, and of the polymer density distribution across the brush [33]. Szleifer et al. provided the theoretical framework for modelling chemical equilibria in weak polyelectrolyte layers on planar and curved surfaces [34], [35]. Examples discussed in these studies [34], [35] include acid-base equilibria, redox equilibria of electroactive brushes, ligand-receptor binding in brushes modified with biological receptors, and the grafting equilibrium of polymer chains with an end-group that can bind to a surface. A key feature identified for all these systems is the different chemical reactivity within the brush as compared to that of isolated polymer chains in solution [34], [35]. Okrugin et al. applied the Scheutjens-Fleer self-consistent field (SF-SCF) numerical theory to investigate the equilibrium properties of strong and weak polyelectrolyte brushes under electrical fields in both salt-free and salt-containing solutions [36]. Computer simulations revealed further details on the brush structure and conformational dynamics [37], the response to external triggers [38],[39], and the interactions with charged macromolecules and (bio)nanocolloids [40], [41].

Besides the development of the theoretical framework, physico-chemical properties of neutral and charged polymer brushes have been largely analyzed by multiscale methods such as contact angle measurements [42], ellipsometry [43], surface plasmon resonance [44], atomic force microscopy [45], electrochemical impedance spectroscopy [46], X-ray reflectivity [47], and neutron scattering techniques [48], and many of the ensuing data could be satisfactorily interpreted by theory.

The optimization of the performance of polyelectrolyte brushes necessarily includes the analysis of the interrelations between the brush charge, structure, and interactions under application-relevant conditions. To achieve this goal, the continuous development of soft surface electrokinetics theories [49], [50], [51], [52], [53], [54] provided the basis for the analysis of intertwined electrostatic and structural properties of polymer brushes. Applying electrokinetic-based methodologies, it was demonstrated how the combined evaluation of streaming current and surface conductivity measurements enables the comprehensive characterization of the interfacial charging, ion binding, and segment density distribution of neutral or charged polymer brushes.

In this article, we briefly review the theory for the electrohydrodynamics of planar soft interfaces exhibiting an inhomogeneous material density distribution. To demonstrate how streaming current and surface conductivity data collected over a wide range of electrolyte concentrations and pH values of the adjacent electrolyte allow for detailed insights into the

brush charge and structure, we present and discuss recent results for poly(ethylene oxide) (PEO) and poly(2-(methacryloyloxy)ethyltrimethylammonium chloride) (PMETAC) brushes. The case of glycosaminoglycan (GAG) brushes is further discussed with the focus on the importance of ion hydration, ion pairing, and dielectric decrement that play a significant role in crowded macromolecular environments.

2 Theoretical framework for interpretation of streaming current and surface conductivity measurements at planar diffuse soft interfaces.

The theoretical framework for the electrohydrodynamics of planar diffuse soft interfaces was developed by Duval et al. [50], [51], [55], [53]. The theory is applicable without limitations on the mathematical nature of the function capturing the segment density distribution, on the film thickness and charge density of the soft polymer film and it was extended for soft multi-layered surface coatings by the same authors [56]. Here, we briefly review the governing electrostatic and hydrodynamic equations used for the interpretation of streaming current and surface conductivity measurements at polymer brushes.

Streaming current and surface conductivity measurements are typically performed across rectangular microchannels formed by identically coated planar sample carriers of length L_o, width l and separation distance H [53]. To ensure laminar flow and to minimize effects of the side walls, the inequalities $H << l$ and $H << L_o$ [53] apply. Furthermore, the thickness of the polymer coating d is considered to be much smaller than H. For further details we refer to Ref. [53].

2.1 Hydrodynamic Flow Field

The hydrodynamic flow field in the microchannel formed by the sample carriers can be calculated according to the generalized Brinkman equation [57]:

$$\frac{d^2V(X)}{dX^2} - (l_o H)^2 f(X) V(X) = -1 \qquad (1)$$

In Eq. (1), X is the normalized spatial coordinate perpendicular to the sample surfaces, $X = x/H$, V the normalized flow velocity, $V(X) = v(X)/v_o$ with $v_o = DPH^2/(hL_o)$ and η the dynamic viscosity of the electrolyte solution, $1/\lambda_o$ the Brinkman length, and $f(X)$ a function that adequately represents the polymer segment distribution of the hydrated polymer film [50]. The latter can be obtained from polymer theories [58] or from data collected by

surface analytical techniques [59],[60],[61]. As demonstrated in Ref. [50], the gradual decrease of the segment density within soft surface layers towards the solutions phase can be adequately modeled using a parameterizable hyperbolic tangent function. If the channel walls are formed by identically coated sample carriers, it is sufficient to solve Eq. (1) from $X = 0$ to $X = 1/2$.

2.2 Electrostatic Potential

The presence of ionized groups or preferentially adsorbed ions at the supporting substrate and/or within the soft polymer film impacts on the electrostatic potential $y(x)$ across the interface. It can be evaluated applying the non-linear Poisson-Boltzmann (PB) equation. For polymer films bearing *M* types of ionizable groups, the equation can be written in the form [55]:

$$\frac{\mathrm{d}^2 y(X)}{\mathrm{d}X^2} = -\frac{(kH)^2}{\sum_{i=1}^{N} c_i z_i^2}\left[\sum_{i=1}^{N} z_i c_i \mathrm{e}^{-z_i y(X)} + \sum_{j=1}^{M} \frac{r_j / F}{1 + 10^{-e_j(\mathrm{p}K_j - \mathrm{pH})}\mathrm{e}^{e_j y(X)}} f(X)\right] \qquad (2)$$

where y is the dimensionless electrostatic potential $(y = Fy / RT)$, κ^{-1} the Debye length, c_i the concentration of the ion species i of valence z_i with $i = 1,...,N$, F the Faraday constant, R the gas constant, and T the temperature. In the numerator of the second term on the right-hand side of Eq. (2), $\left|r_{j=1,...,M}\right| / F$ stands for the total concentration of ionizable groups of type *j* within the film [55]. The ionization of these groups is characterized by their associated pK_j value. The parameter e_j in Eq. (1) is -1 for the ionization of functional groups due to deprotonation reactions and +1 for ionization of groups due to protonation reactions [55]. In case of more complex charge formation processes, additional terms can be added to the right-hand side of Eq. (2).

2.3 Streaming current

Combining the expressions for the hydrodynamic flow field (1) and the electrostatic potential (2), the streaming current I_{str} caused by the hydrodynamic transport of counter ions along the channel walls is given by:

$$\frac{I_{\mathrm{str}}}{DP} = \frac{2\mathrm{l}FH^3}{hL_{\mathrm{o}}}\int_0^{1/2}\sum_{i=1}^{N} z_i c_i \mathrm{e}^{-z_i y(X)} V(X)\mathrm{d}X \qquad (3)$$

The streaming current can be directly measured for given pressure differences ΔP across the channel using reversible electrodes (typically Ag/AgCl) positioned at both sides of the streaming channel [53].

2.4 Surface conductivity

The accumulation of mobile counter ions within and at the soft polymer film causes an elevated conductivity at the surfaces forming the streaming channel, designated as surface conductivity, K^{σ} [62]. It involves contributions due to the migration of ions, K_{m}^{σ}, and due to the electroosmotic ion transport, K_{eo}^{σ}, in the tangential electrical field $U_{\mathrm{str}} / L_{\mathrm{o}}$, arising from the streaming potential U_{str} across the microchannel [53]. The total surface conductivity is therefore given by [53]:

$$K^{\sigma} = K_{\mathrm{m}}^{\sigma} + K_{\mathrm{eo}}^{\sigma} \tag{4}$$

with

$$K_{\mathrm{m}}^{\sigma} = \frac{HF^2}{RT} \int_0^{1/2} \sum_{i=1}^{N} |z_i| D_i c_i b_i(X) \left(e^{-z_i y(X)} - 1 \right) dX \tag{5}$$

and

$$K_{\mathrm{eo}}^{\sigma} = \frac{H \varepsilon_{\mathrm{o}} \varepsilon_{\mathrm{r}} RT (kH)^2}{h} \int_0^{1/2} V_{\mathrm{eo}}(X) \sum_{i=1}^{N} z_i c_i e^{-z_i y(X)} dX \tag{6}$$

where D_i is the diffusion coefficient of ion species i in the bulk electrolyte, $b_i(X)$is the position dependent ratio of the diffusion coefficient of ion i at position X and that in the bulk electrolyte, and $\varepsilon_o \varepsilon_r$ is the dielectric permittivity of the medium. For highly hydrated polymer films, we it is reasonable to assume $b_i(X) \approx 1$ [49]. The electroosmotic flow field $V_{\mathrm{eo}}(X)$ can be calculated using the Brinkman equation (1) after substituting the right-hand side by the relevant charge source term [51].

Experimentally, the total surface conductivity of the polymer/solution interface can be determined by measuring the streaming current, I_{str}, the streaming potential, U_{str}, at different pressures DP across the microchannel, and the bulk electrolyte conductivity, K^{B}, applying the following equation [63]:

$$\frac{I_{\mathrm{str}} / DP}{U_{\mathrm{str}} / DP} \frac{L_{\mathrm{o}}}{2l} = \frac{H}{2} K^{\mathrm{B}} + K^{\sigma} \tag{7}$$

Highest accuracy is achieved in determining K^{σ} for experimental conditions where the *Dukhin* number $Du = K^{\sigma} / \left(K^{B} H \right) \geq 1$.

3 Charging and structure of polymer brushes unraveled by combined streaming current and surface conductivity analysis

During the past decade, the experimental approaches and the theoretical framework outlined above were successfully applied to characterize electrically neutral and polyelectrolyte brushes. In the following sections, we review and discuss illustrative studies that demonstrate how combined evaluation of streaming current and surface conductivity lead to quantitative evaluation of brush charge and structure under different aqueous medium conditions.

3.1 Combined self-consistent field and soft surface electrokinetic theories to unravel the segment density distribution in PEO brushes

Poly(ethylene oxide) (PEO) is a hydrophilic polymer that exhibits low non-specific interactions with proteins and other biomacromolecules. Accordingly, PEO brushes are widely used in the fields of biomedical and environmental engineering to e.g. reduce biofouling [64]. The propensity of PEO brushes to inhibit/limit this undesired side effect is intimately connected with the brush architecture [64],[65].

To characterize the charging and segment distribution of PEO brushes, Zimmermann et al. [58] combined the self-consistent field (SCF) theory [24] with the theory for the electrohydrodynamics at planar diffuse soft interfaces [53] to interpret streaming current measurements. The PEO brushes were prepared with a grafting density of $\sigma = 0.1$ nm^{-2} on polystyrene (PS) coated glass substrates using a Langmuir-Blodgett technique [66]. The used PEO-PS block copolymer consisted of a PEO block with in average 700 monomer units (denoted here as N_{av}) and a PS block of 38 repeat units. The latter was used to tightly anchor the polymer chains at the PS-coated substrate [66]. The SCF theory [24] was applied to calculate the segment density distribution of the PEO brushes using the known polydispersity of PD = 1.25 [58]. For the sake of comparison, profiles for a monodisperse brush (PD = 1) and a brush with a homogeneous density of polymer segments (box model) [21],[23] were considered in this study as well [58] (Fig. 1).

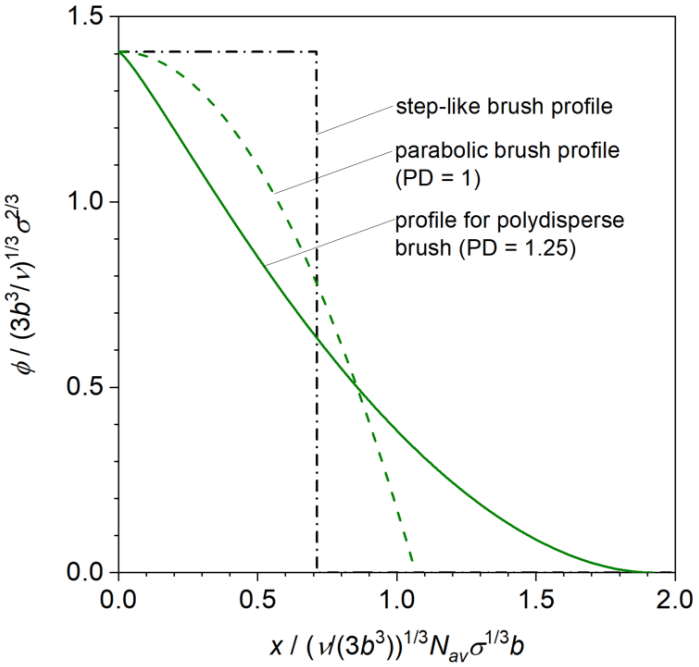

Fig. 1: Dimensionless density profiles calculated according to the SCF theory for PEO brushes with a polydispersity (PD) of 1 and 1.25 in the direction *x* normal to substrate surface. For reference purposes, a step-like profile for a brush with homogeneous polymer segment density (box profile) is shown as well. For further details concerning profile calculation we refer to Refs. [24] and [58]. Reprinted with permission of the Royal Society of Chemistry from Zimmermann R, Romeis D, Bihannic I, Cohen Stuart M, Sommer JU, Werner C, Duval JFL Electrokinetics as an alternative to neutron reflectivity for evaluation of segment density distribution in PEO brushes. Soft Matter 2014;10:7804-7809, Copyright 2014; permission conveyed through Copyright Clearance center, Inc.

Streaming current measurements at pure PS films in the pH range between 9.5 and 3 of a 1 mM KCl solution (Fig. 2A) revealed that the interfacial charging at the PS substrate is caused by unsymmetrical adsorption of water ions [58],[67]. Under the given pH and electrolyte conditions, the streaming current measured for the PEO brush grafted to the PS was found to be significantly lower than that for pure PS film (Fig. 2A). This feature suggests that the hydrodynamic flow at the PS/solution interface is significantly suppressed by the presence of the uncharged PEO chains. The position of the isoelectric points close to pH 4 and the minor differences between surface conductivities [68] as measured for the bare and PEO-grafted PS surfaces further indicated that the interfacial charging by unsymmetrical adsorption of hydroxide and hydronium ions at the PS surface is not significantly altered by the presence of the PEO brush [58]. Measurements as a function of salt concentration (Fig. 2B) showed the typical *electrokinetic fingerprint* of electrostatic charge screening and the

limited hydrodynamic transport of the counter ions located within the electrically neutral PEO coating that compensate the PS surface charge [50]. The magnitude of the streaming current strongly decreased with the salt concentrations in the range between 0.01 and 1 mM due to the increasing hydrodynamic screening of the counter ions in the brush and approached asymptotically to zero at higher salt concentrations (Fig. 2B).

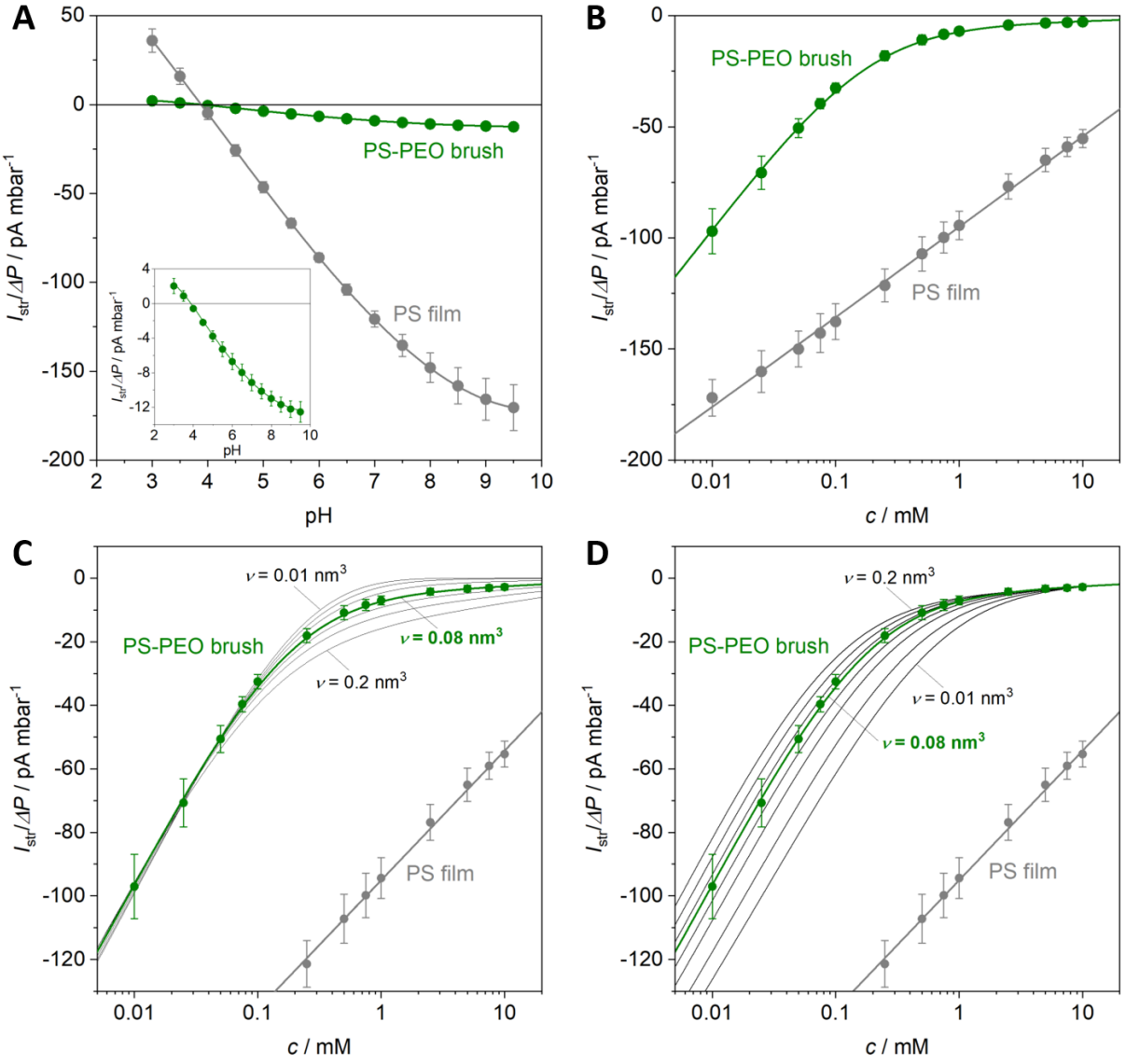

Fig. 2: Streaming current vs. pressure gradient, I_{str}/DP, measured upon varying pH of a 1 mM KCl solution (A, insert of A: data are zoomed) and with varying KCl solution concentrations (denoted as c) at pH = 6 (B) for the bare PS-coated substrate (grey) and the PEO brush (green) grafted to the PS film. Symbols represent experimental data and solid lines simulation curves obtained from combined SCF and soft surface electrokinetic theories with adopting the brush profile estimated for PD = 1.25 (Fig. 1) and an excluded PEO monomer unit volume of ν = 0.08 nm^3. The strategy for the determination of the couple (ν,1/λ_o) is

illustrated in panels C and D. The streaming current data were fitted in the range of low electrolyte concentrations (C), where I_{str}/DP depends linearly on the logarithm of *c*, and in the range of high electrolyte concentrations (D), where I_{str}/DP gradually tends to a zero value, for fixed values of the excluded volume parameter ν between 0.01 and 0.2 nm^3 (see Refs. [69], [70], [71], [72]) by sole adjustment of the hydrodynamic penetration length $1/\lambda_o$ according to least mean square method. The couple (ν,$1/\lambda_o$) obtained for the best fit of the data was ν = (0.08 ± 0.01) nm^3 and $1/\lambda_o$ = (15.5 ± 0.1) nm. Other model parameters: PD = 1.25, b = 0.37 nm, σ = 0.1 nm^{-2}, N_{av} = 700, *z* = 1, *T* = 295.15 K, ε_r =79.5 (relative dielectric permittivity of the medium), η = 0.954 mPa s, *H* = 30 μm, l = 10 mm, and L_o = 20 mm. Adapted with permission of the Royal Society of Chemistry from Zimmermann R, Romeis D, Bihannic I, Cohen Stuart M, Sommer JU, Werner C, Duval JFL Electrokinetics as an alternative to neutron reflectivity for evaluation of segment density distribution in PEO brushes. Soft Matter 2014;10:7804-7809, Copyright 2014; permission conveyed through Copyright Clearance center, Inc.

To interpret the streaming current data shown in Fig. 2A and B, the dimensionless brush profile obtained for PD = 1.25 was converted into the real segment density distribution [58] and subsequently used for the calculation of the hydrodynamic flow field (function $f(X)$ in Eq. (1)). In this series of simulations, the excluded volume ν of the PEO monomer unit was the only unknown parameter together with the Brinkman length, $1/\lambda_o$, and both quantities were systematically varied for best fitting the streaming current data for all electrolyte concentrations (Fig. 2C and D). We would like to emphasize that the variation of ν has a direct impact on the PEO segment density distribution and accordingly strongly affects the hydrodynamic flow field, which in turn modulates the magnitude of the streaming current (Eq. 3) (it is recalled that PEO material is uncharged). The experimental data were best reproduced with ν = (0.08 ± 0.01) nm^3, which agreed remarkably with ν data published in literature [69], [70], [71], [72]. The minor differences were attributed by the authors of this study [58] to the approximations underlying the validity of the mean-field Poisson-Boltzmann equation [50], [51], [53]. The obtained Brinkman length $1/\lambda_o$ that reflects flow penetration into the PEO brush was 15.5 ± 0.1 nm (green curves in Fig. 2C and D). The consistency of the approach was further verified by adopting the values ν = 0.08 nm^3 and $1/\lambda_o$ = 15.5 nm to compute the dependence of the streaming current on pH in 1 mM KCl electrolyte. The theoretical predictions compared very well to measurements performed at varying pH values

in 1 mM KCl (Fig. 2A). Attempts to reproduce the streaming current data using the (non-realistic) parabolic and box profiles did not allow quantitative matching between experiment and theory [58]. Furthermore, applying the theory developed by Fermon [73], the authors showed that the subtle differences in the segment density distribution in the tail region of the PEO brush could not be resolved by neutron reflectivity technique [58].

More recently, the approach was successfully applied for the interpretation of streaming current measurements at PEO brushes featuring a pronounced anti-fouling character [74]. The brushes were obtained by end-tethering of heterobifunctional PEOs (Mn ≈ 20 000 g mol^{-1}) to polydopamine (PDA) modified surfaces, the latter causing the interfacial charge by ionization of the PDAs functional groups [74]. Similar to the results shown in Fig. 2A and B for the PS/PEO system, the charge of the PDA was hydrodynamically screened by the grafted PEO chains. Streaming current data measured for the PEO brushes at different electrolyte concentrations and pH values were reproduced by theory and used to determine the segment density profile distribution [74] in a way similar to that detailed above for PS/PEO brush.

Overall, the interfacial charging and structure of PEO brushes were comprehensively characterized by the analysis of streaming current data measured over a wide range of pH values and electrolyte concentrations with combined self-consistent field and soft surface electrokinetic theories. For highly hydrated systems with low volume fractions of the polymer chains in the tail region, the introduced methodology is a relevant alternative to unresolved neutron reflectivity measurements for a proper evaluation of the spatial brush density profile.

3.2 Ion-pairing in cationic brushes revealed by analyses of streaming current and surface conductivity

Polyelectrolytes provide versatile options for the formation of polymer brushes that are tunable in structure, space charge density, wettability, and adhesiveness by external triggers [1], [42], [75]. Profound understanding of correlations between the charge and structure is crucial for the optimization of the brush performance under given medium conditions. Below, we review recent work on the electrokinetic analysis of the structure, interfacial, and bulk charging of poly(2-(methacryloyloxy)ethyltrimethylammonium chloride) (PMETAC) brushes, and on the electrokinetics-based analysis of ion-pairing in this system [76]. In contrast to the analysis presented above for PEO brushes, the approach requires the independent determination of the brush thickness *d*, e.g. by ellipsometry, under the experimental conditions used for electrokinetic and surface conductivity measurements.

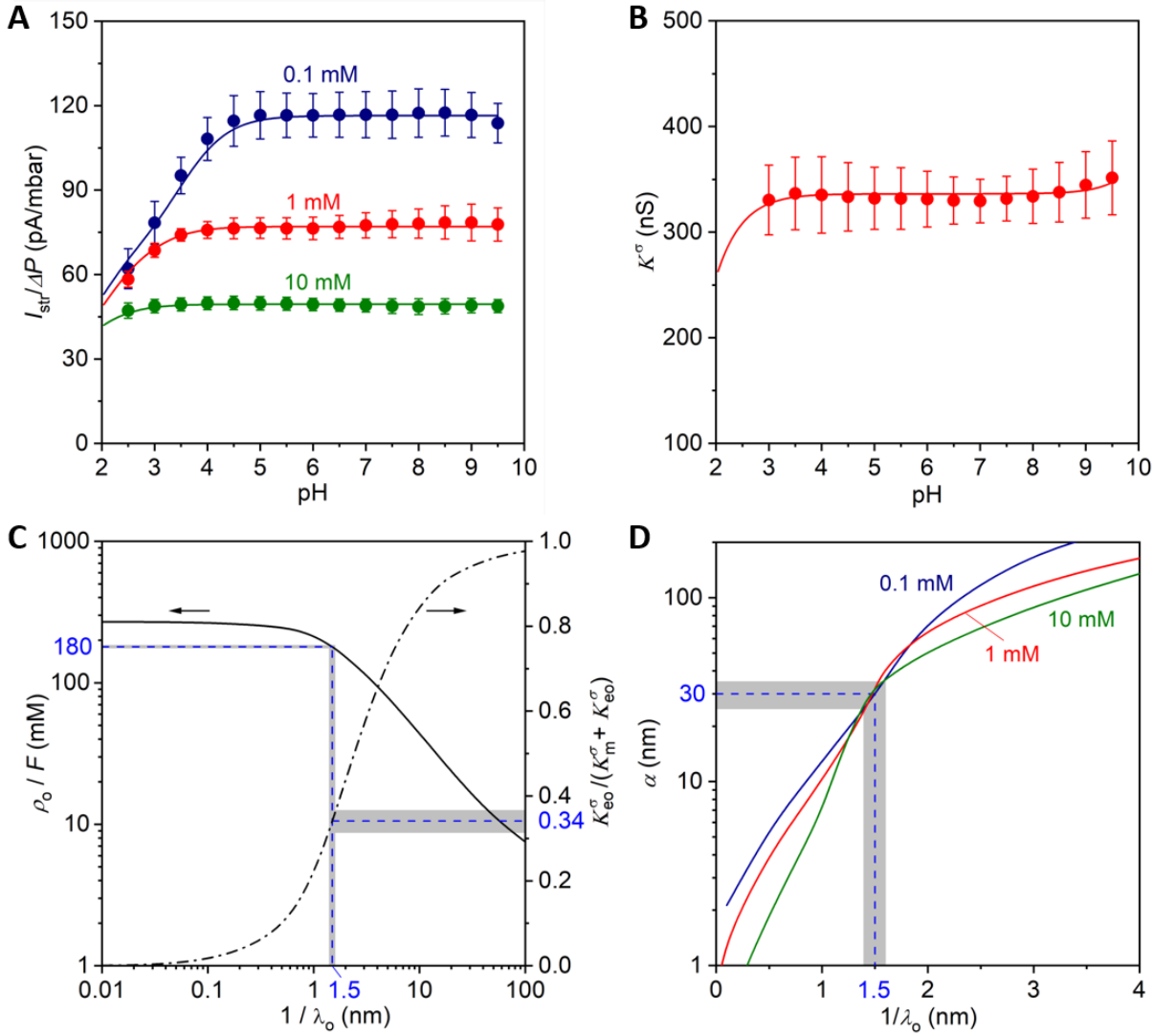

Fig. 3: (A) Streaming current vs. pressure gradient, I_{str}/DP, measured for PMETAC brushes at varying pH values of 0.1 mM, 1 mM, and 10 mM KCl solutions. (B) Surface conductivity, K^{σ}, of the brush/electrolyte solution interphase at varying pH values of a 1 mM KCl solution. Symbols represent experimental data and solid lines simulation curves obtained on the basis of soft surface electrokinetic theory. (C) Concentration of ionizable groups in the brush, r_o/F (left), and contribution of electroosmosis to the total surface conductivity, $K^{\sigma}_{eo}/(K^{\sigma}_{m}+K^{\sigma}_{eo})$ (right), vs. Brinkman length, $1/l_o$, for the $(r_o/F, 1/l_o)$ couples that best reproduce the K^{σ} vs. pH data shown in panel B. (D) Interface diffuseness, a, vs. Brinkman length, $1/l_o$, for 0.1 mM, 1 mM and 10 mM KCl solutions. The best fit of the streaming current and surface conductivity data shown in (A) and (B) was obtained with r_o/F = (180 ± 5) mM, $1/l_o$ = (1.5 ± 1) nm, and a = (30 ± 5) nm. In panels C and D, the range of parameters r_o/F, $1/l_o$ and a used for the consistent interpretation of all streaming current and surface

conductivity data displayed in A and B is highlighted in grey. Other model parameters: d = 160 nm (obtained from ellipsometry). Adapted with permission from Zimmermann R, Gunkel-Grabole G, Bünsow J, Werner C, Huck WTS, Duval JFL. Evidence of Ion-Pairing in Cationic Brushes from Evaluation of Brush Charging and Structure by Electrokinetic and Surface Conductivity Analysis. The Journal of Physical Chemistry C. 2017;121:2915-22. Copyright 2017 American Chemical Society.

The permanent positive brush charge (as expected from the quaternary ammonium groups of the PMETAC) was reflected by the positive streaming current vs. pH curves measured in 0.1 mM, 1 mM, and 10 mM KCl solutions (Fig. 3A). In line with theory, variations of the streaming current with salt concentration were observed and resulted from an increase of PMETAC charge screening with increasing solution ionic strength (in the low pH range, both protons and background electrolyte ions contribute significantly to solution ionic strength) [76]. The nearly pH-invariant surface conductivity of 330 nS measured in 1 mM KCl solution underpinned the permanent cationic character of the PMETAC brush (Fig. 3B). The minor variations of K^{σ} with pH result from the nature of charge compensation operational in the brush with changing electrolyte composition [76]. Quantitative interpretation of the streaming current and surface conductivity data revealed a charge density of r_o / F = (180 ± 5) mM, corresponding to 66% of migrative and 34% electroosmotic transport contributions to the total surface conductivity (Fig. 3C). The diffuseness of the PMETAC/solution interface (which basically represents the decay length of the tanh-like polymer segment density distribution at the very interface formed with the external electrolyte solution) and the Brinkman length were found to be (30 ± 5) nm and (1.5 ± 1) nm, respectively (Fig. 3D).

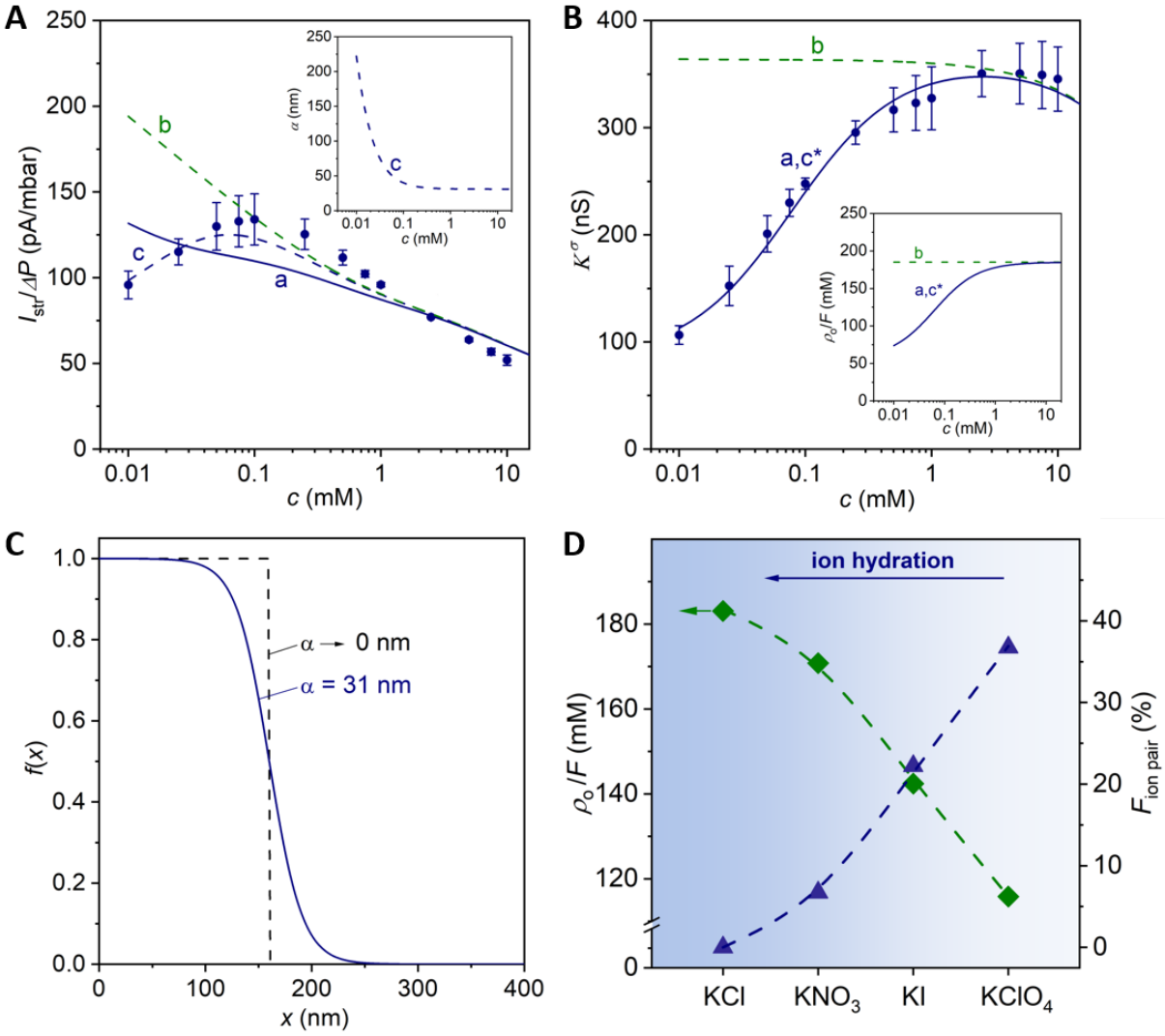

Fig. 4: (A) Streaming current vs. pressure gradient, I_{str}/DP, and (B) surface conductivity, K^{σ}, for PMETAC brushes (circles) measured at varying KCl solution concentrations *c* (pH = 6). The surface conductivity data (B) were reproduced by theory considering a reduction of the brush net charge density due to ion pairing (solid line). The reduction of the brush charge density did not allow the reconstruction of the streaming current data (solid line (a) in panel A) at low KCl concentrations. Instead, I_{str}/DP was reproduced by increasing the interfacial diffuseness α for constant brush charge density (blue dashed lines (c) in panel A and in the inset of A). The green dashed lines in A and B represent simulations relevant for a brush with constant charge density and constant interfacial diffuseness (r_o/F = 185 mM, α = 31 nm). Curves (a) and (c*) in B were obtained for a brush with variable net charge density (due to ion pairing, see inset) and either α = 31 nm (a) or variable α (c*) with salt concentration *c*, as shown in the inset of A. The superposition of curves (a) and (c*) in panel B illustrates that the interfacial diffuseness α has no impact on the surface conductivity. (C) Segment density distribution in the brush for α = 0 nm and *a* = 31 nm calculated for *d* = 160 nm (as obtained

from ellipsometry). For the computation of I_{str}/DP and K^{σ} (solid lines in A and B, respectively), α = 31 nm was used. Please note that similar profiles (obtained for α = (30 ± 5) nm)) were used to reproduce the complete set of data shown in Fig. 3A and B, thus ensuring consistency of data analyses versus pH (Fig. 3) and salt concentration (Fig. 4). (D) Concentration of ionized sites, r_o/F, and fraction of quaternary ammonium groups forming pairs with anions, $F_{\text{ion pair}}$, in 1 mM KCl, KNO_3, KI and $KClO_4$ electrolyte solutions. Adapted with permission from Zimmermann R, Gunkel-Grabole G, Bünsow J, Werner C, Huck WTS, Duval JFL. Evidence of Ion-Pairing in Cationic Brushes from Evaluation of Brush Charging and Structure by Electrokinetic and Surface Conductivity Analysis. The Journal of Physical Chemistry C. 2017;121:2915-22. Copyright 2017 American Chemical Society.

The measurement and analysis of the streaming current and surface conductivity at varying KCl solution concentrations between 0.01 mM and 10 mM (pH = 6) provided further details on the brush structure. The streaming current increased at low salt concentrations, reached a maximum at 0.1 mM, and decreased at higher salt concentrations (Fig. 4A). The surface conductivity showed a similar dependence on salt concentration with the occurrence of a maximum of ~350 nS at 3 mM KCl (Fig. 4B). A consistent quantitative interpretation of both data sets was achieved considering distinct physical origins of the maxima in the streaming current and surface conductivity with varying electrolyte concentration [76]. In agreement with previous work of Chu et al. [77], the association between counter ions and the quaternary ammonium groups was identified as the origin for the decrease of the density of ionized sites in the brush (parameter r_o/F) and the accompanied decrease in surface conductivity at low salt concentrations (Fig. 4B). The formation of ion pairs between the counter ions and quaternary ammonium groups was found to lead to a reduction of the charge density with about 60 % of occupied (charge neutralized) ammonium groups in 0.01 mM KCl solution. In the next step, streaming current data were reproduced by increasing the interfacial diffuseness (inset of Fig. 4A) for a salt-invariant concentration of ionized groups (r_o/F = 185 mM). This, at the first glance contradictory result can be explained by the fact that both techniques probe the charge and structure within different regions of diffuse soft interfaces: The streaming current is very sensitive to charge and structure in the electrokinetic active brush region located at the very film/electrolyte solution interphase [53]. Unlike streaming current, the surface conductivity probes the conductive and electroosmotic ion transports within the whole soft surface layer and it is rather insensitive to the very electrostatic and

structural features of the outermost layer region (the electrokinetically active zone) that are reflected in the streaming current [53]. Being aware of these fundamental principles, it was concluded from both data sets that ion pairing, chain hydration, multiplet formation [78], [79], and brush swelling are different in the peripheral and inner regions of the brush probed by streaming current and surface conductivity, respectively. Interestingly, Zhao et al. observed a similar characteristic for the outer region of sodium polystyrene sulfonate brushes by neutron reflectivity measurements [80].

Zimmermann et al. [76] further analyzed the ion paring of different chaotropic anions in 1 mM KCl, KNO_3, KI, and $KClO_4$ solutions (Fig. 4D). The anion binding was found to increase in the order: $Cl^- < NO_3^- < I^- < ClO_4^-$. Compared to the 1 mM KCl solution, the fraction of charge-neutralized quaternary ammonium groups ($F_{\text{ion pair}} = (1- r_o / r_{o,KCl}) \cdot 100\%$) was 7% in 1 mM KNO_3, 22% in 1 mM KI and 37% in 1 mM $KClO_4$ solution, that is, the formation of ion pairs increased with the hydrophobicity of the anions (Fig. 4D). In line with previous work [81],[42], the brush adapted its original charge after replacing the tested solutions by 1 mM KCl [76].

Altogether, the example illustrates how the combined evaluation of streaming current and surface conductivity data provides quantitative information on the charge state, structure, and ion-pairing of polyelectrolyte brushes. These findings provide a basis for understanding, predicting and modulating the properties of polyelectrolytes in aqueous environments and their interactions with neighboring (bio)colloidal particles.

3.3 Emerging theory: Ion pairing, brush dielectric decrement, and born forces on ions

The anion binding to PMETAC brushes described in the previous section shows the expected ion-pair ordering based on *Collin's Rule of matching water affinities* [82], [83]. This rule describes the trend that ion pairing is preferred for similarly hydrated ion pairs more than for differently hydrated ions. This tendency for ion pairing in a brush can be made by considering the local concentration of unpaired fixed charges of the brush and unpaired counterions in solution to drive the ion pair complex by the law of mass action. This formulation introduces an overall dissociation constant, $k_{ij,}$ defined as the product of the concentrations of the unpaired ions divided by the local concentration of ion pairs. An overall dissociation constant is a combination of intermediate populations of solvent separated ion pairs as described by Marcus and Hefter [84] and originally introduced by Eigen and Tamm [85]. Thus, the effect of ion pairing can be captured upon extension of the classical formulation of mean field PB Eq. (2) by replacing the pH dependent term to represent ion-

pairing rather than protonation of unbound fixed brush charges. This approach was applied by Sterling and Baker to estimate the ion pair dissociation constants of PMETAC brush quaternary amine pairing to the various anions [86].

In addition to the hydration-dependent ion pairing modifications to the PB model, recent findings have led to two additional important hydration-related effects that could be considered to accurately model ion behavior in polyelectrolyte brushes. Both effects are based on the reduced dielectric constant of water within the brush. The brush charged molecules and the associated counterions are hydrated with *vicinal* water molecules that are not as free to rotate as when constrained only by hydrogen-bonding with other water molecules. The dielectric constant is therefore variable [87]. An ion competes for water molecules that are within more-constrained or less-constrained environments. The result is a so-called Born force that drives ions to regions of lower dielectric constant [88]. The dimensionless Born energy of an ion, $B(X)$, as it moves from the saline solution with relative permittivity e_s to a brush region with relative permittivity $e(X)$ can be written,

$$B(X) = \frac{-\Delta G_i^s}{k_B T}\frac{e_w}{e_w - 1}\left(\frac{1}{e(X)} - \frac{1}{e_s}\right) \tag{8}$$

where ΔG_i^s is the hydration free energy of ion i and e_w the relative permittivity of pure water [89]. This position-dependent permittivity $e(X)$ can be specified by considering the dependence upon all local molecular constituents, but it is often described using a Maxwell mixture formula based on local ions only. With inclusion of this effect, the ion partitioning term can be written as follows:

$$c_i(X) = c_{i,o}\exp\{-z_i y(X) - B(X)\} \tag{9}$$

Accordingly, the dimensionless PB equation extended for ion pairing and position-dependent dielectric permittivity becomes

$$\frac{d^2 y(X)}{dX^2} + \frac{dy(X)}{dX}\frac{de_r(X)}{dX} = -\frac{(kH)^2}{\sum_{i=1}^{N} c_{i,o} z_i^2}\left[\sum_{i=1}^{N} z_i c_i(X) + \sum_{j=1}^{M}\frac{z_j c_{j,o}(X)}{1+\sum_{i=1}^{N}\frac{c_i(X)}{k_{ij}}}\right] \tag{10}$$

where the index i represents mobile ions and the index j represents brush fixed charges, and k_{ij} is the dissociation constant of ion binding between mobile ions and fixed brush charges that must be specified. Note that the derivative of the dielectric permittivity with respect to space in the left-hand side of Eq. (10) is already included in the generic formulation of the mean field PB equation, but is often negligible in dilute *in vitro* environments because the

permittivity is nearly invariant with position. However, a lower permittivity, or *dielectric decrement* occurs as molecular crowding hinders water movement within a brush. Concluding, Eq. (10) includes three modifications to Eq. (2): modification of the brush charges by ion pair equilibria represented by k_{ij}, ion partitioning due to both electrostatic and Born hydration gradients associated with dielectric decrement (Eq. 8), and the usual dielectric decrement term from Poisson's equation on the left side of Eq. (10).

Example of glycosaminoglycan brushes simulated with all-atom molecular dynamics

The hydration-related effects mentioned above and included in the modified PB Eq. (10) are important for macromolecular interactions in biological environments. For example, the application of PB models for chondroitin sulfate GAG brushes under high-resolution force spectroscopy was developed without these effects [28]. However, results obtained from molecular dynamic (MD) simulations for heparin and hyaluronic acid brushes highlight that there can indeed be a delicate balance between electrostatic and hydration effects that require inclusion of these effects within the PB framework [90]. In this work, all-atom MD simulations revealed that hyaluronan and oversulfated heparin brushes in NaCl and KCl show an important switch of behavior between the two cations Na^+ and K^+ that results from their different water affinities [90].

The all-atom simulations of tethered heparin brushes in 200 mM NaCl and KCl demonstrated that Born hydration energy and ion-pairing energy can be of the same order of magnitude as electrostatic energy in these crowded macromolecular environments. These simulations made use of an array of 4 strands of 16-disaccharide glycans tethered at their midpoint where $Z = 0$ was defined. (Note that the authors use Z as the axis that is perpendicular to the brush-solution interface rather than X as defined above.) Periodic boundary conditions in directions along the brush surface resulted in an infinite brush of a 20Å × 20Å array of glycans that were each ~160 Å long when fully extended (because each disaccharide is ~10Å long). Simulations were performed using CHARMM36 with force fields of recent NBFIX corrections for cation interactions with carboxylates and sulfates of the brush.

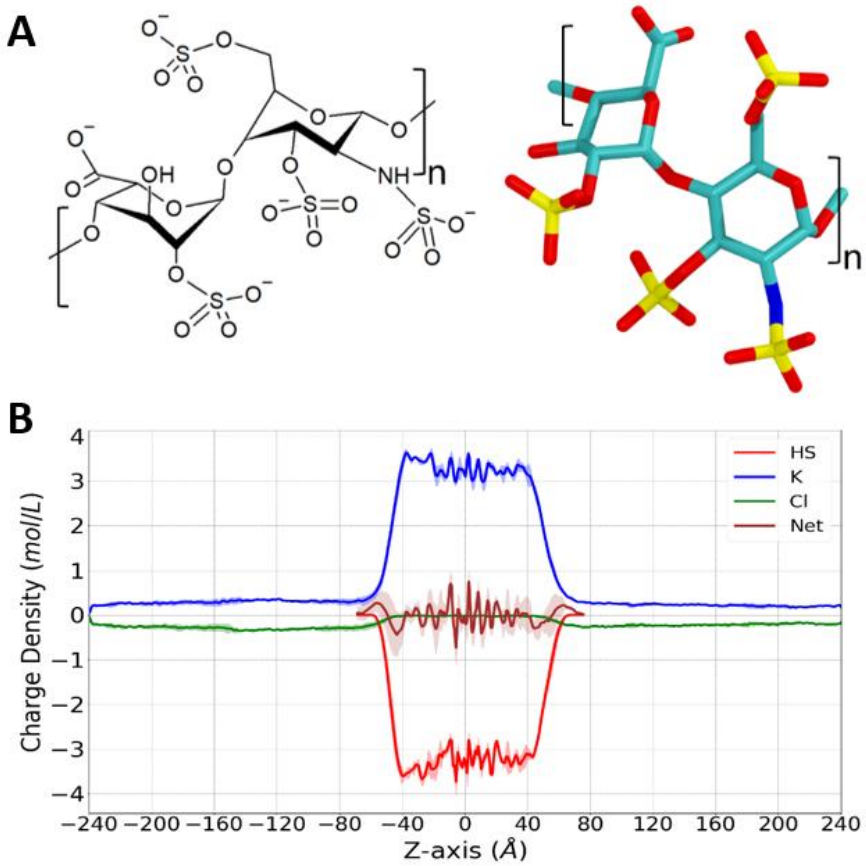

Fig. 5: (A) Molecular structure of oversulfated heparin glycosaminoglycan disaccharide GlcA2Sα4GlcNS3S6Sα4. Sixteen of these repeating units make a polysaccharide strand. (B) Strands tethered on a 20Å × 20Å grid make a brush that is seen to be about 120 Å thick in the plot of the X-Y averaged charge density. The simulation used 23,724 water molecules, 413 cations, and 93 chloride ions. Adapted with permission from Sterling JD, Jiang W, Botello-Smith WM, Luo YL. Ion Pairing and Dielectric Decrement in Glycosaminoglycan Brushes. The Journal of Physical Chemistry B. 2021;125:2771-80. Copyright 2021 American Chemical Society.

Simulations were launched with fully-extended glycans that were observed to collapse to a statistically-invariant length of about 80% of the initial length after about 70 ns. The average charge density of the brush is seen in Fig. 5B to be about 3M concentration of the anionic sulfates and carboxylate charges in the brush (red curve) and electroneutrality is achieved by partitioning of an equal concentration of potassium shown in the blue curve. The chloride ions (green) are seen to be excluded from the brush region and electroneutrality outside the brush is seen as the blue/green curve balance.

The MD simulation results can be used compute the permittivity of water $e(X)$, and here it was observed to be ~38 in the glycocalyx brush and ~60 outside. Using this result, the

difference in Born-hydration energy of ions was estimated using Eq. (8). The ion-hydration energies were published values of ΔG^{s}_{Na} = -424 kJ/mol and ΔG^{s}_{K} = -352 kJ/mol. The electrostatic potential y_b was computed using the particle-Mesh Ewald (PME) algorithm.

Table 1: Cation partition energies from heparin brush all-atom simulations. The residual cation binding energy was determined as the difference between column 2 values and the sum of column 3 and 4 values.

Salt	Total Partitioning Energy of Cation / k_BT	PME Brush Electrostatic Potential Energy $\frac{Fy_b}{RT}$	Cation Born Hydration Energy Difference $\frac{-\Delta G_i^s}{k_BT}\frac{e_w}{e_w-1}\left(\frac{1}{e(X)}-\frac{1}{e_s}\right)$	Cation Binding Energy $\frac{\Delta\mu_i}{k_BT}$
NaCl	-2.34	-0.62±0.27	1.62±0.6	-3.35±0.6
KCl	-2.41	0.96±0.14	1.36±0.5	-4.73±0.5

Remarkably, ***the heparin brush electrostatic potential energy was observed to be negative when sodium is present but is positive with potassium***. This result demonstrates ion-specific behavior with similar biophysics as in potassium ion-channels that reject sodium ions because of their tight/large hydration shell [91]. The spacing of oxygens associated with sulfates and carboxylates appear to mimic the tight spacing of oxygen atoms within potassium ion channels. Although the brush displays net electroneutrality, the cations move readily between the anionic brush charges with temporary pairing in contact ion pairing (CIP) and solvent-separated ion pairing (SIP) whose combined effects are represented through quantification of either ion-pair dissociation constants as shown in Eq. (10), or through the residual binding energy as given in Table 1. The cation binding energy formalism is not consistent with the law of mass action formulation of ion pairing shown in Eq. (10) but is a useful estimate for the ion pairing energy.

As potassium sheds its hydration shell more easily, the net ion-pairing energy with glycan anions is greater than with sodium, consistent with Collins' Rule of matching water affinities. Thus, a positive electrostatic potential difference is actually needed for potassium in the heparin brush to reach electroneutrality. The criterion for the brush to attain a positive electrostatic potential can be written as

$$\ln\left(\frac{c_{i,b}}{c_{i,o}}\right)+\frac{-\Delta G_i^s}{k_BT}\frac{e_w}{e_w-1}\left(\frac{1}{e_b}-\frac{1}{e_s}\right)+\frac{Dm_i}{k_BT}<0 \qquad (11)$$

Consider a brush that has higher charge density than the solution such that the first term in Eq. (11) is positive. Electroneutrality requires that if there is strong ion-pairing (large negative Dm_i) and low hydration energy (small negative ΔG_i^S) the organization of charges and dipoles must yield a surprisingly positive electrostatic potential within the anionic brush. This behaviour highlights the important interplay between the hydration energy that always drives ions away from the crowded brush while ion pairing attracts ions into the brush. These effects are important for the heparin brush with a charge density of ~3M, but vanish in the dilute polymer limit with the standard Donnan-partitioning of ions limit being recovered at sufficiently low ion and brush charge densities.

4. Conclusions and perspectives.

End-grafting of polymers is a widely applied and versatile method to tune the surface properties of bulk materials. Significant progress in understanding the formation and properties of polymer brushes was achieved by the development of polymer theories and the broad application of surface-sensitive characterization methods. In this article, we provide the fundamentals for analysing experimentally obtained streaming current and surface conductivity data applying the theory on the electrohydrodynamics at planar diffuse soft interfaces. Illustrative examples demonstrate the application of the methodology to obtain a quantitative understanding on the interrelations between brush charging and structure in aqueous electrolytes. In particular, we review and discuss in details the benefits of combining SCF and soft surface electrokinetic theories for a precise evaluation of the segment distribution within PEO brushes, a feature that is not possible from conventional neutron reflectivity measurements on diluted polymer layer samples. As an example for deciphering the interplay between charging and structural features of polymer brushes, we review and discuss data for strong cationic PMETAC brushes, including data for binding chaotropic anions as employed for dynamic regulation of wettability [42]. Within the assumptions underlying the applicability of the mean-field Poisson-Boltzmann equation [62] and considering the differentiated polymer brush zones probed by streaming current and surface conductivity measurements [53], [63], the options arising from the recent theoretical developments enable a holistic characterisation of interfacial charging and structure of polymer brushes on planar surfaces. Analogous concepts were provided by Duval and collaborators [92],[93] for the electrohydrodynamics of diffuse soft particles. The theoretical framework provided in Ref. [92] constitutes the basis for interpreting electrophoretic mobilities of polymer brush grafted particles.

Biointerfaces, such as the mammalian cell glycocalyx, can be investigated based on concepts developed and applied for studies on synthetic polyelectrolyte brushes. Living matter is molecularly crowded such that dielectric decrement appears in the form of Born hydration gradient forces on ions and as effective charges that modify, together with ion pairing, the electrostatic potential distribution. Modifications of the Poisson-Boltzmann formulation that capture these effects are presented herein.

Future extensions of the methodology involve the combination between SCF and molecular-scale theories for charged brushes with implementation of relevant equations for the ionic transports along the brush-electrolyte interface. The exploitation of streaming current and surface conductivity data collected on polyampholytic polymer layers and brushes with unique tuneable properties [94], [95] necessarily requires the extension of the theoretical framework for systems containing multiple types of ionizable groups that dynamically interact with each other and with electrolyte ions upon changes of the electrolyte composition. The field could further benefit from increased sensitivity and data modelling of complementary surface analytical techniques such as small-angle neutron scattering [96] and terahertz time-domain spectroscopy [97] that directly probe structural features of soft surface layers and polymers in solution, respectively.

5. CRediT author statement

Zimmermann, Ralf: Conceptualization, Writing - Original Draft, Visualization
Duval, Jerome F. L.: Writing - Review & Editing
Werner, Carsten: Writing - Review & Editing
Sterling, James: Writing - Original Draft, Visualization

6. Conflict of interest declaration

The authors declare that they have no competing interests.

7. References

[1] Azzaroni O. Polymer brushes here, there, and everywhere: Recent advances in their practical applications and emerging opportunities in multiple research fields. Journal of Polymer Science Part A: Polymer Chemistry. 2012;50:3225-58.
[2] Ma S, Zhang X, Yu B, Zhou F. Brushing up functional materials. NPG Asia Materials. 2019;11.
[3] Li M, Pester CW. Mixed Polymer Brushes for "Smart" Surfaces. Polymers (Basel). 2020;12.
[4] Brittain WJ, Minko S. A structural definition of polymer brushes. Journal of Polymer Science Part A: Polymer Chemistry. 2007;45:3505-12.
[5] Chen W-L, Cordero R, Tran H, Ober CK. 50th Anniversary Perspective: Polymer Brushes: Novel Surfaces for Future Materials. Macromolecules. 2017;50:4089-113.
[6] Kobayashi M, Terayama Y, Yamaguchi H, Terada M, Murakami D, Ishihara K, et al. Wettability and antifouling behavior on the surfaces of superhydrophilic polymer brushes. Langmuir. 2012;28:7212-22.
[7] Zhulina EB, Rubinstein M. Lubrication by Polyelectrolyte Brushes. Macromolecules. 2014;47:5825-38.
[8] Suriyanarayanan S, Lee HH, Liedberg B, Aastrup T, Nicholls IA. Protein-resistant hyperbranched polyethyleneimine brush surfaces. J Colloid Interface Sci. 2013;396:307-15.
[9] Emilsson G, Schoch RL, Feuz L, Hook F, Lim RY, Dahlin AB. Strongly stretched protein resistant poly(ethylene glycol) brushes prepared by grafting-to. ACS Appl Mater Interfaces. 2015;7:7505-15.
[10] Yan S, Luan S, Shi H, Xu X, Zhang J, Yuan S, et al. Hierarchical Polymer Brushes with Dominant Antibacterial Mechanisms Switching from Bactericidal to Bacteria Repellent. Biomacromolecules. 2016;17:1696-704.
[11] Li D, Xu L, Wang J, Gautrot JE. Responsive Polymer Brush Design and Emerging Applications for Nanotheranostics. Adv Healthc Mater. 2021;10:e2000953.
[12] Badoux M, Billing M, Klok H-A. Polymer brush interfaces for protein biosensing prepared by surface-initiated controlled radical polymerization. Polymer Chemistry. 2019;10:2925-51.
[13] Giussi JM, Cortez ML, Marmisolle WA, Azzaroni O. Practical use of polymer brushes in sustainable energy applications: interfacial nanoarchitectonics for high-efficiency devices. Chem Soc Rev. 2019;48:814-49.
[14] Chen T, Ferris R, Zhang J, Ducker R, Zauscher S. Stimulus-responsive polymer brushes on surfaces: Transduction mechanisms and applications. Progress in Polymer Science. 2010;35:94-112.
[15] Adiga SP, Brenner DW. Stimuli-Responsive Polymer Brushes for Flow Control through Nanopores. J Funct Biomater. 2012;3:239-56.
[16] Kieviet BD, Schon PM, Vancso GJ. Stimulus-responsive polymers and other functional polymer surfaces as components in glass microfluidic channels. Lab Chip. 2014;14:4159-70.
[17] Conrad JC, Robertson ML. Towards mimicking biological function with responsive surface-grafted polymer brushes. Current Opinion in Solid State and Materials Science. 2019;23:1-12.
[18] Boyaciyan D, Krause P, von Klitzing R. Making strong polyelectrolyte brushes pH-sensitive by incorporation of gold nanoparticles. Soft Matter. 2018;14:4029-39.
[19] Das S, Banik M, Chen G, Sinha S, Mukherjee R. Polyelectrolyte brushes: theory, modelling, synthesis and applications. Soft Matter. 2015;11:8550-83.
[20] Currie EPK, Norde W, Cohen Stuart MA. Tethered polymer chains: surface chemistry and their impact on colloidal and surface properties. Advances in Colloid and Interface Science. 2003;100-102:205-65.

[21] Alexander S. Adsorption of chain molecules with a polar head a scaling description. Journal de Physique. 1977;38:983-7.
[22] de Gennes PG. Scaling theory of polymer adsorption. Journal de Physique. 1976;37:1445-52.
[23] de Gennes PG. Conformations of Polymers Attached to an Interface. Macromolecules. 1980;13:1069-75.
[24] Milner ST, Witten TA, Cates ME. Theory of the grafted polymer brush. Macromolecules. 2002;21:2610-9.
[25] Wijmans CM, Scheutjens JMHM, Zhulina EB. Self-consistent field theories for polymer brushes: lattice calculations and an asymptotic analytical description. Macromolecules. 2002;25:2657-65.
[26] Milner ST. Strong-stretching and Scheutjens–Fleer descriptions of grafted polymer brushes. J Chem Soc, Faraday Trans. 1990;86:1349-53.
[27] Netz RR, Schick M. Polymer Brushes: From Self-Consistent Field Theory to Classical Theory. Macromolecules. 1998;31:5105-22.
[28] Dean D, Seog J, Ortiz C, Grodzinsky AJ. Molecular-Level Theoretical Model for Electrostatic Interactions within Polyelectrolyte Brushes: Applications to Charged Glycosaminoglycans. Langmuir. 2003;19:5526-39.
[29] Chen CM, Fwu YA. Monte Carlo simulations of polymer brushes. Phys Rev E Stat Nonlin Soft Matter Phys. 2001;63:011506.
[30] Bedrov D, Smith GD. Molecular dynamics simulation study of the structure of poly(ethylene oxide) brushes on nonpolar surfaces in aqueous solution. Langmuir. 2006;22:6189-94.
[31] Pincus P. Colloid stabilization with grafted polyelectrolytes. Macromolecules. 1991;24:2912-9.
[32] Zhulina EB, Birshtein TM, Borisov OV. Theory of Ionizable Polymer Brushes. Macromolecules. 1995;28:1491-9.
[33] Zhulina EB, Borisov OV. Poisson-Boltzmann theory of pH-sensitive (annealing) polyelectrolyte brush. Langmuir. 2011;27:10615-33.
[34] Nap RJT, M.; Gonzalez Solveyra, E.; Ren, C.L.; Uline, M.J.; Szleifer, I. Modeling of Chemical Equilibria in Polymer and Polyelectrolyte Brushes. Polymer and Biopolymer Brushes: John Wiley & Sons; 2017.
[35] Gonzalez Solveyra E, Nap RJ, Huang K, Szleifer I. Theoretical Modeling of Chemical Equilibrium in Weak Polyelectrolyte Layers on Curved Nanosystems. Polymers (Basel). 2020;12.
[36] Okrugin BM, Richter RP, Leermakers FAM, Neelov IM, Zhulina EB, Borisov OV. Electroresponsive Polyelectrolyte Brushes Studied by Self-Consistent Field Theory. Polymers. 2020;12.
[37] Santos DES, Li D, Ramstedt M, Gautrot JE, Soares TA. Conformational Dynamics and Responsiveness of Weak and Strong Polyelectrolyte Brushes: Atomistic Simulations of Poly(dimethyl aminoethyl methacrylate) and Poly(2-(methacryloyloxy)ethyl trimethylammonium chloride). Langmuir. 2019;35:5037-49.
[38] Rodriguez-Ropero F, van der Vegt NF. Ionic specific effects on the structure, mechanics and interfacial softness of a polyelectrolyte brush. Faraday Discuss. 2013;160:297-309; discussion 11-27.
[39] Sachar HS, Chava BS, Pial TH, Das S. All-Atom Molecular Dynamics Simulations of the Temperature Response of Densely Grafted Polyelectrolyte Brushes. Macromolecules. 2021;54:6342-54.
[40] Yigit C, Kanduc M, Ballauff M, Dzubiella J. Interaction of Charged Patchy Protein Models with Like-Charged Polyelectrolyte Brushes. Langmuir. 2017;33:417-27.

[41] Laktionov MY, Zhulina EB, Borisov OV. Proteins and Polyampholytes Interacting with Polyelectrolyte Brushes and Microgels: The Charge Reversal Concept Revised. Langmuir. 2021;37:2865-73.
[42] Azzaroni O, Brown AA, Huck WTS. Tunable Wettability by Clicking Counterions Into Polyelectrolyte Brushes. Advanced Materials. 2007;19:151-4.
[43] Rauch S, Uhlmann P, Eichhorn KJ. In situ spectroscopic ellipsometry of pH-responsive polymer brushes on gold substrates. Anal Bioanal Chem. 2013;405:9061-9.
[44] Ferrand-Drake del Castillo G, Emilsson G, Dahlin A. Quantitative Analysis of Thickness and pH Actuation of Weak Polyelectrolyte Brushes. The Journal of Physical Chemistry C. 2018;122:27516-27.
[45] Xu X, Billing M, Ruths M, Klok HA, Yu J. Structure and Functionality of Polyelectrolyte Brushes: A Surface Force Perspective. Chem Asian J. 2018;13:3411-36.
[46] Motornov M, Sheparovych R, Katz E, Minko S. Chemical gating with nanostructured responsive polymer brushes: mixed brush versus homopolymer brush. ACS Nano. 2008;2:41-52.
[47] Kesal D, Christau S, Trapp M, Krause P, von Klitzing R. The internal structure of PMETAC brush/gold nanoparticle composites: a neutron and X-ray reflectivity study. Phys Chem Chem Phys. 2017;19:30636-46.
[48] Kilbey SM, Ankner JF. Neutron reflectivity as a tool to understand polyelectrolyte brushes. Current Opinion in Colloid & Interface Science. 2012;17:83-9.
[49] Yezek LP, Duval JFL, van Leeuwen HP. Electrokinetics of diffuse soft interfaces. III. Interpretation of data on the polyacrylamide/water interface. Langmuir. 2005;21:6220-7.
[50] Duval JFL, Zimmermann R, Cordeiro AL, Rein N, Werner C. Electrokinetics of diffuse soft interfaces. IV. Analysis of streaming current measurements at thermoresponsive thin films. Langmuir. 2009;25:10691-703.
[51] Zimmermann R, Kuckling D, Kaufmann M, Werner C, Duval JFL. Electrokinetics of a poly(N-isopropylacrylamid-co-carboxyacrylamid) soft thin film: evidence of diffuse segment distribution in the swollen state. Langmuir. 2010;26:18169-81.
[52] Barbati AC, Kirby BJ. Soft diffuse interfaces in electrokinetics – theory and experiment for transport in charged diffuse layers. Soft Matter. 2012;8.
[53] Zimmermann R, Dukhin SS, Werner C, Duval JFL. On the use of electrokinetics for unraveling charging and structure of soft planar polymer films. Current Opinion in Colloid & Interface Science. 2013;18:83-92.
[54] Duval JFL, Werner C, Zimmermann R. Electrokinetics of soft polymeric interphases with layered distribution of anionic and cationic charges. Current Opinion in Colloid & Interface Science. 2016;24:1-12.
[55] Duval JFL, Kuttner D, Nitschke M, Werner C, Zimmermann R. Interrelations between charging, structure and electrokinetics of nanometric polyelectrolyte films. J Colloid Interface Sci. 2011;362:439-49.
[56] Duval JFL, Kuttner D, Werner C, Zimmermann R. Electrohydrodynamics of soft polyelectrolyte multilayers: point of zero-streaming current. Langmuir. 2011;27:10739-52.
[57] Brinkman HC. A calculation of the viscous force exerted by a flowing fluid on a dense swarm of particles. Appl Sci Research. 1947;A1:27-34.
[58] Zimmermann R, Romeis D, Bihannic I, Cohen Stuart M, Sommer JU, Werner C, et al. Electrokinetics as an alternative to neutron reflectivity for evaluation of segment density distribution in PEO brushes. Soft Matter. 2014;10:7804-9.
[59] Toomey R, Freidank D, Rühe J. Swelling Behavior of Thin, Surface-Attached Polymer Networks. Macromolecules. 2004;37:882-7.
[60] Sanjuan S, Perrin P, Pantoustier N, Tran Y. Synthesis and swelling behavior of pH-responsive polybase brushes. Langmuir. 2007;23:5769-78.

[61] Junk MJ, Anac I, Menges B, Jonas U. Analysis of optical gradient profiles during temperature- and salt-dependent swelling of thin responsive hydrogel films. Langmuir. 2010;26:12253-9.
[62] Lyklema J. Fundamentals of Interface and Colloid Science. Vol. II: Solid-Liquid Interfaces. London: Academic Press; 1995.
[63] Zimmermann R, Duval JFL, Werner C. On the analysis of ionic surface conduction to unravel charging processes at macroscopic soft and hard solid–liquid interfaces. Current Opinion in Colloid & Interface Science. 2019;44:177-87.
[64] Hucknall A, Rangarajan S, Chilkoti A. In Pursuit of Zero: Polymer Brushes that Resist the Adsorption of Proteins. Advanced Materials. 2009;21:2441-6.
[65] Bernhard C, Roeters SJ, Franz J, Weidner T, Bonn M, Gonella G. Repelling and ordering: the influence of poly(ethylene glycol) on protein adsorption. Phys Chem Chem Phys. 2017;19:28182-8.
[66] Currie EPK, Van der Gucht J, Borisov OV, Stuart MAC. Stuffed brushes: theory and experiment. Pure and Applied Chemistry. 1999;71:1227-41.
[67] Zimmermann R, Freudenberg U, Schweiß R, Küttner D, Werner C. Hydroxide and hydronium ion adsorption — A survey. Current Opinion in Colloid & Interface Science. 2010;15:196-202.
[68] Zimmermann R, Norde W, Cohen Stuart MA, Werner C. Electrokinetic characterization of poly(acrylic acid) and poly(ethylene oxide) brushes in aqueous electrolyte solutions. Langmuir. 2005;21:5108-14.
[69] Xu R, Winnik MA, Riess G, Chu B, Croucher MD. Micellization of polystyrene-poly(ethylene oxide) block copolymers in water. 5. A test of the star and mean-field models. Macromolecules. 2002;25:644-52.
[70] Devanand K, Selser JC. Asymptotic behavior and long-range interactions in aqueous solutions of poly(ethylene oxide). Macromolecules. 2002;24:5943-7.
[71] Dormidontova EE. Role of Competitive PEO−Water and Water−Water Hydrogen Bonding in Aqueous Solution PEO Behavior. Macromolecules. 2002;35:987-1001.
[72] Lonetti B, Tsigkri A, Lang PR, Stellbrink J, Willner L, Kohlbrecher J, et al. Full Characterization of PB−PEO Wormlike Micelles at Varying Solvent Selectivity. Macromolecules. 2011;44:3583-93.
[73] Fermon C. La réflectivité de neutrons. Le Journal de Physique IV. 2001;11:Pr9-33-Pr9-66.
[74] Pop-Georgievski O, Zimmermann R, Kotelnikov I, Proks V, Romeis D, Kucka J, et al. Impact of Bioactive Peptide Motifs on Molecular Structure, Charging, and Nonfouling Properties of Poly(ethylene oxide) Brushes. Langmuir. 2018;34:6010-20.
[75] Hsu JP, Yang ST, Lin CY, Tseng S. Voltage-controlled ion transport and selectivity in a conical nanopore functionalized with pH-tunable polyelectrolyte brushes. J Colloid Interface Sci. 2019;537:496-504.
[76] Zimmermann R, Gunkel-Grabole G, Bünsow J, Werner C, Huck WTS, Duval JFL. Evidence of Ion-Pairing in Cationic Brushes from Evaluation of Brush Charging and Structure by Electrokinetic and Surface Conductivity Analysis. The Journal of Physical Chemistry C. 2017;121:2915-22.
[77] Chu X, Yang J, Liu G, Zhao J. Swelling enhancement of polyelectrolyte brushes induced by external ions. Soft Matter. 2014;10:5568-78.
[78] Kou R, Zhang J, Wang T, Liu G. Interactions between Polyelectrolyte Brushes and Hofmeister Ions: Chaotropes versus Kosmotropes. Langmuir. 2015;31:10461-8.
[79] Kramarenko EY, Philippova OE, Khokhlov AR. Polyelectrolyte networks as highly sensitive polymers. Polymer Science Series C. 2006;48:1-20.

[80] Zhao B, Yuan G, Chu X, Yang J, Zhao J. Response of a Permanently Charged Polyelectrolyte Brush to External Ions: The Aspects of Structure and Dynamics. Langmuir. 2018;34:6757-65.
[81] Huang CJ, Chen YS, Chang Y. Counterion-activated nanoactuator: reversibly switchable killing/releasing bacteria on polycation brushes. ACS Appl Mater Interfaces. 2015;7:2415-23.
[82] Collins KD. The behavior of ions in water is controlled by their water affinity. Q Rev Biophys. 2019;52:e11.
[83] Roy S, Baer MD, Mundy CJ, Schenter GK. Marcus Theory of Ion-Pairing. J Chem Theory Comput. 2017;13:3470-7.
[84] Marcus Y, Hefter G. Ion pairing. Chem Rev. 2006;106:4585-621.
[85] Eigen MT, K. Schallabsorption in Elektrolytlösungen als Folge chemischer Relaxation I. Relaxationstheorie der mehrstufigen Dissoziation. Zeitschrift für Elektrochemie, Berichte der Bunsengesellschaft für physikalische Chemie. 1962;66:93-107.
[86] Sterling JD, Baker SM. Electro-lyotropic equilibrium and the utility of ion-pair dissociation constants. Colloid and Interface Science Communications. 2017;20:9-11.
[87] Gavish N, Promislow K. Dependence of the dielectric constant of electrolyte solutions on ionic concentration: A microfield approach. Phys Rev E. 2016;94:012611.
[88] Mahapatra P, Gopmandal PP, Duval JFL. Effects of dielectric gradients- mediated ions partitioning on the electrophoresis of composite soft particles: An analytical theory. Electrophoresis. 2021;42:153-62.
[89] Boda D, Henderson D, Gillespie D. The role of solvation in the binding selectivity of the L-type calcium channel. J Chem Phys. 2013;139:055103.
[90] Sterling JD, Jiang W, Botello-Smith WM, Luo YL. Ion Pairing and Dielectric Decrement in Glycosaminoglycan Brushes. J Phys Chem B. 2021;125:2771-80.
[91] Kuang Q, Purhonen P, Hebert H. Structure of potassium channels. Cell Mol Life Sci. 2015;72:3677-93.
[92] Duval JFL, Ohshima H. Electrophoresis of diffuse soft particles. Langmuir. 2006;22:3533-46.
[93] Beaussart A, Caillet C, Bihannic I, Zimmermann R, Duval JFL. Remarkable reversal of electrostatic interaction forces on zwitterionic soft nanointerfaces in a monovalent aqueous electrolyte: an AFM study at the single nanoparticle level. Nanoscale. 2018;10:3181-90.
[94] Haag SL, Bernards MT. Polyampholyte Hydrogels in Biomedical Applications. Gels. 2017;3.
[95] Ramirez R, Woodcock J, Kilbey SM. ARGET-ATRP synthesis and swelling response of compositionally varied poly(methacrylic acid-co-N,N-diethylaminoethyl methacrylate) polyampholyte brushes. Soft Matter. 2018;14:6290-302.
[96] Wei Y, Hore MJA. Characterizing polymer structure with small-angle neutron scattering: A Tutorial. Journal of Applied Physics. 2021;129.
[97] Serin G, Nguyen HH, Marty JD, Micheau JC, Gernigon V, Mingotaud AF, et al. Terahertz Time-Domain Spectroscopy of Thermoresponsive Polymers in Aqueous Solution. J Phys Chem B. 2016;120:9778-87.

Annotations for references:

[34] ** Molecular theory for different chemical equilibria in polyelectrolyte brushes.

[35] * Theoretical methods and illustrative examples for modelling weak polyelectrolytes at curved interfaces.

[36] * Self-consistent field numerical approach to study equilibrium properties of tethered strong and weak polyelectrolytes with either immobilized surface charge or applied electrical field.

[58] ** Combination of electrohydrodynamic and self-consitent field theory to analyze the segment distribution in polymer brushes.

[74] * Modelling of streaming current data for poly(ethylene oxide) brushes on polydopamine-functionalized surfaces using electrohydrodynamic and self-consistent field theory.

[76] ** Analysis of surface conductivity measurements provides insights into ion pairing in cationic polymer brushes.

[82] ** Comphrehensive review on the hydration of ions in water and related effects in biological systems.

[88] * Analytical theory for the electrophoresis of core–shell particles defined by various combinations of hydrodynamic and electrostatic properties pertaining to their core and shell components and with full account of dielectric-induced ions partitioning effects.

[90] ** All-atom molecular dynamics simulations of glycoseaminoglycane brushes. Concept to account for ion pairing, brush dielectric decrement, and born forces on ions.

[97] * Terahertz Time-Domain Spectroscopy to study the hydration of polymers under crowding conditions.